

REPORT NO. NADC-84054-60



CHARACTERIZATION OF NEWLY DEVELOPED CONDUCTIVE COMPOSITES

L. J. Buckley, I. Shaffer, R. Trabucco
Aircraft and Crew Systems Technology Directorate
NAVAL AIR DEVELOPMENT CENTER
Warminster, PA 18974

MARCH 1984

FINAL REPORT
P.E. 6276IN
WF61-542

100% QUANTITY INSPECTED 2

Approved for Public Release; Distribution Unlimited

Prepared for
NAVAL AIR SYSTEMS COMMAND
Department of the Navy
Washington, DC 20361

19970605 018
810 60090766

8400384

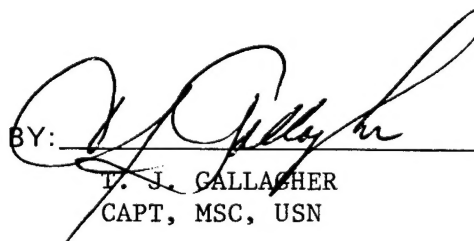
NOTICES

REPORT NUMBERING SYSTEM – The numbering of technical project reports issued by the Naval Air Development Center is arranged for specific identification purposes. Each number consists of the Center acronym, the calendar year in which the number was assigned, the sequence number of the report within the specific calendar year, and the official 2-digit correspondence code of the Command Office or the Functional Directorate responsible for the report. For example: Report No. NADC-78015-20 indicates the fifteenth Center report for the year 1978, and prepared by the Systems Directorate. The numerical codes are as follows:

CODE	OFFICE OR DIRECTORATE
00	Commander, Naval Air Development Center
01	Technical Director, Naval Air Development Center
02	Comptroller
10	Directorate Command Projects
20	Systems Directorate
30	Sensors & Avionics Technology Directorate
40	Communication & Navigation Technology Directorate
50	Software Computer Directorate
60	Aircraft & Crew Systems Technology Directorate
70	Planning Assessment Resources
80	Engineering Support Group

PRODUCT ENDORSEMENT – The discussion or instructions concerning commercial products herein do not constitute an endorsement by the Government nor do they convey or imply the license or right to use such products.

APPROVED BY:



T. J. GALLAGHER
CAPT, MSC, USN

DATE:

9 August 1984

UNCLASSIFIED

SECURITY CLASSIFICATION OF THIS PAGE (When Data Entered)

20. ABSTRACT (Continued)

noting fiber distribution, orientation and fracture morphology. A laser diffraction technique was used to determine the degree of orientation. Electrical conductivities (DC Resistance Method) were obtained for various samples. Physical properties such as water absorption, water vapor transmission, and chemical resistance have also been determined.

S/N 0102- LF- 014- 6601

UNCLASSIFIED

TABLE OF CONTENTS

	<u>Page</u>
LIST OF TABLES	ii
LIST OF FIGURES	ii
INTRODUCTION	1
MATERIALS	1
EXPERIMENTAL PROCEDURE	2
ELECTRICAL PROPERTIES	2
ELECTROCHEMICAL MEASUREMENTS	2
MOISTURE ABSORPTION AND CHEMICAL RESISTANCE	2
TENSILE AND IMPACT PROPERTIES	3
MICROSCOPY AND ORIENTATION STUDIES	3
RESULTS AND DISCUSSION	3
PHYSICAL AND ELECTRICAL PROPERTIES	3
MECHANICAL PROPERTIES AND MICROSCOPY	4
SUMMARY	5
FUTURE EFFECTS	5
REFERENCES	22
ACKNOWLEDGEMENTS	22

NADC-84054-60

LIST OF TABLES

<u>Table</u>		<u>Page</u>
I	Operational and Maintenance Chemicals	6
II	Electrical and Electrochemical Properties	6
III	Tensile and Impact Properties of Chopped Fiber Filled PPS and PEI	7

LIST OF FIGURES

<u>Figure</u>		<u>Page</u>
1	Plot of EMI Attenuation (vs. frequency) Comparing Nickel Plated Plated PPS (40% Gr), uncoated PPS (40% Gr), and Aluminum	8
2	Comparison of Galvanic Couples (40% Gr/PPS vs. Acrylic) Exposed to Salt Fog	9
3	Effects of the Three Harshest Solvents After One Week Immersion	10
4	Plots of Water Absorption vs. Time for Various Composites	11
5	Force vs. Time Plots of Several Drop-Weight Impact Tests for Gr/PPS (10%, 20%, 30% and 40% Gr)	12
6	SEM Photographs of 20% Gr/PPS and PEI Tensile Fracture Surfaces (1000X)	13
7	Force vs. Time Plots of 40% Gr and NiGr PPS from Drop-Weight Impact Tests	14
8	SEM Photographs of 40% Gr and NiGr/PPS Tensile Fracture Surfaces (2000X)	15
9	Photomicrographs (50X) of 20% and 30% Gr/PEI	16
10	Photomicrographs (50X) of 20% and 30% Gr/PPS	17
11	Photomicrograph (50X) of 40% Gr/PPS	18
12	Laser Diffraction Patterns for 20% and 40% Gr/PPS	19
13	Series of Laser Diffraction Patterns Corresponding to Various Levels of Orientation	20
14	SEM Photograph of NiGr Fibers on the As-Molded Surface (200X)	21

INTRODUCTION

New aircraft designs are always seeking to exploit the advantages posed by composite materials. Much has been said about the superior mechanical properties and significant weight savings to be realized. These properties can be directly translated into aircraft performance parameters such as increased range, improved flight capabilities, and greater payload. The general trend in military and to some extent commercial aircraft is to use polymer matrix composites in a greater proportion of the airframe.

Most applications of composites have been with continuous graphite, Kevlar, or glass fiber in epoxy matrices. These materials make up the bulk of typical airframe composite components found on fixed and rotary wing aircraft. However significant payoffs are attainable by using discontinuous fiber reinforced thermoplastics⁽¹⁾. With inherent processing advantages, thermoplastics are amenable to mass production manufacturing methods such as injection and compression molding. These methods are fast and relatively inexpensive in comparison to other methods such as autoclave processing. Filling the thermoplastic with a suitable fiber such as glass or graphite imparts enhanced strength and stiffness to the material⁽²⁾.

Modern aircraft employ a number of small metallic components such as electrical connectors, avionics enclosures, and fittings. These components, because of their metallic nature, are vulnerable to corrosion. This naturally occurring process accounts for tremendous expenditures in maintenance dollars. Because of the great number on the aircraft, the weight of these components is also a disadvantage. Metallic components have an inherent advantage in that they naturally provide some measure of electromagnetic interference (EMI) attenuation by preventing interference between electrical signals.

Thermoplastics filled with conductive reinforcements offer a significant level of EMI shielding.^(3,4) Typically chopped graphite fibers are used, but additional benefits are possible with the use of more highly conducting reinforcements such as metallized graphite and stainless steel. This effort was undertaken to develop such materials and establish the potential for their application on naval aircraft. A number of graphite and metallized graphite reinforced thermoplastics were characterized with regard to specific mechanical and electrical properties for this study. Data was generated from injection molded plaques and specimens.

MATERIALS

All of the matrix materials used for this work were injection moldable thermoplastics. A solvent resistance test screening was performed initially on six of the systems. These systems were*: 30% NiGr/Nylon 66; 30% Gr/PEI; 12% SS/PPO; 35% AL FL/Nylon 66; 7% SS/PC; and 40% Gr/PPS. The stainless steel filled samples at the time were only available with PC and PPO. It was understood that these polymers would not have the best chemical resistance. Liquid crystalline polyester (LCP) with 40% Gr type 2330 from Celanese was also investigated. Due to the good solvent resistance and elevated temperature capability PPS# and PEI were chosen for further evaluation. The high elongation PPS (PPS#) was used for all tests after the initial solvent screening. PPS with 10%, 20%, 30%, and 40% by weight chopped graphite fibers and nickel coated chopped graphite fibers was acquired. PEI with 10%, 20%, and 30% by weight chopped graphite fibers was also acquired. Plaques of PPS with 50% and 60% NiGr were obtained for electrical measurements. Material was received as molded tensile specimens and plaques from LNP (Malvern, PA); RTP (Winona, MN); and Wilson-Fiberfil (Evansville, IN).

* Gr	- Graphite
NiGr	- Nickel Coated Graphite
PEI	- Polyetherimide
SS	- Stainless Steel (Type 301)
PPO	- Polyphenylene Oxide
AL FL	- Aluminum Flake
PC	- Polycarbonate
PPS	- Polyphenylene Sulfide
PPS#	- High Elongation PPS

EXPERIMENTAL PROCEDURE

ELECTRICAL PROPERTIES

Resistivity measurements were conducted on the materials molded into plaques and tensile bars. EMI measurements were made solely on the plaques.

Volume resistivity measurements were made according to ASTM D257-76 across the thickness of the sheet material. A kelvin bridge was used to measure the resistance between copper plates under a pressure of 500 psi.

The attenuation of electromagnetic energy was measured in shielded room tests on nickel plated plaques and unplated plaques.

ELECTROCHEMICAL MEASUREMENTS

The open circuit potential or driving force associated with corrosion reactions was measured with an electrometer or a potentiostat. Measurements were made in a 3.5% sodium chloride solution with a saturated calomel electrode (SCE) as the reference standard. The output of either instrument was connected to a strip chart recorder and the potential was recorded until it became constant (typically one hour).

Corrosion rates displayed by galvanic couples were determined by a zero impedance technique. A potentiostat was used as a zero impedance instrument by appropriate external connections. In this mode composite samples were connected to the working electrode and samples of 7075-T6 aluminum alloy to the reference electrode shorted to the auxiliary electrode. The potentiostat set at 0.000V applied potential allowed the galvanic current to be continuously recorded.

Galvanic corrosion effects were further explored by exposing couples of PPS#/40% Gr and 7075-T6 aluminum in a salt fog chamber in accordance with ASTM test method B117 for one week. Specimens were joined with nylon bolts and nuts and compared to control couples of aluminum and acrylic sheet.

MOISTURE ABSORPTION AND CHEMICAL RESISTANCE

Moisture absorption tests were conducted at 140°F and 95% RH in accordance with ASTM test method D570-63. Small coupons of the plaque materials were used. Chemical resistance tests were performed by immersing small coupons of the composite materials for one week in covered jars containing the different operational and maintenance chemicals commonly used on Navy aircraft. Table I contains a list of these chemicals.

TENSILE AND IMPACT PROPERTIES

Tensile strength, modulus, and strain to failure were done as a quality check for the PPS# and PEI samples. The tensile specimens were tested as received from an end gated injection mold. Center gated plaques were used as drop weight impact specimens. A Dynatup, Model 502, instrumented drop weight impact tester was used.

MICROSCOPY AND ORIENTATION STUDIES

Scanning electron microscopy (SEM) was used to obtain photographs of the tensile fracture surfaces as well as the smooth surfaces. Various samples from the plaques were sectioned, polished, and photographed under 50X magnification. A reduced negative of this photograph was then used as a diffraction mask. A low power helium-neon laser can then be used as a source for generating a diffraction pattern indicative of the overall orientation of the chopped fibers.

RESULTS AND DISCUSSION

PHYSICAL AND ELECTRICAL PROPERTIES

The volume resistivities of the various composite materials are listed in table II. Resistivities were similar for equal loading and fiber type. The nickel plated graphite fibers at 40 volume percent loadings provided the most conductive composites. The measured resistivity for this material was 10^{-1} ohm-cm.

EMI results for PPS + 40 wt % Gr are plotted in figure 1. Composite plaques in the bare and nickel plated condition are compared to a 0.125-inch thick aluminum alloy plate. The uncoated materials showed less attenuation than the aluminum plate at all frequencies except for the low end of the frequency spectrum. The degree of attenuation demonstrated by the aluminum could possibly have been greater at the lower end of the frequency range. The dynamic readings indicate the maximum resolution of the equipment at a particular frequency and the attenuation by the metal is at these levels in some cases. Plating the reinforced thermoplastic brought the attenuation up to the same levels as that of the aluminum.

Open circuit potential measurements were made in this study to show the degree of electrochemical disparity between the reinforced thermoplastics and high strength aluminum alloys commonly used in aircraft structural applications. Previous studies^(5,6) revealed that graphite epoxy composites are galvanically noble materials and tend to actively promote corrosion when fastened to active metals such as aluminum. The results of open circuit potential measurements made in this study are reported in table II. The potential differences of almost 0.9 volts between the aluminum and any of the graphite or stainless steel reinforced materials is relatively large and provide the driving force for accelerated corrosion of the aluminum to occur.

While the open circuit potential readings are used to predict the tendency for galvanic corrosion, they are not a measure of the corrosion rates. A powerful tool for that information is the zero impedance technique. Galvanic corrosion currents are approximated from the corrosion currents which are obtained from polarization diagrams.

Corrosion Current Data obtained from this technique are presented in table II. The data clearly indicate that a galvanic corrosion problem can be expected under suitable conditions when graphite reinforced thermoplastics are coupled to aluminum alloys.

Additional evidence of this problem is found in figure 2 which shows a comparison of the couples exposed in the salt fog chamber. While the aluminum panels in both couples were subjected to pitting corrosion the one coupled to the PPS+40%Gr was more severely corroded as evidenced by the number of pits and the volume of corrosion products.

Figure 3 shows the condition of the composite coupons after one week immersion in the three harshest solvents included in the study. The LCP 2330 which exhibited excellent chemical resistance was a 40% Gr reinforced thermoplastic polymer. Of the other materials evaluated the PPS# and to a lesser degree the PEI polymers demonstrated the best chemical resistance. The PPS# was unaffected by every chemical except the epoxy paint stripper which caused slight dissolution. PEI was severely deteriorated by the epoxy paint stripper and MEK solvent.

The results of the water absorption tests are plotted in figure 4. As expected the Nylon 66 showed the highest absorption values. The other materials showed much lower moisture saturation levels.

MECHANICAL PROPERTIES AND MICROSCOPY

Table III lists the results of the mechanical property tests. The tensile strength and strain to failure for the PEI was much higher than the PPS#. This was also true for the Drop Weight Impact Tests which were based on through penetration and therefore increased as the strength (fiber content) increased. Figure 5 shows force vs. time plots of the different fiber contents in PPS#. The higher fiber contents required more force (for through penetration) but failed in shorter times.

Scanning electron microscopy (SEM) shows in figure 6 a comparison of the PEI and PPS# tensile fracture surfaces with uncoated Gr fibers (20%). The PEI samples show less fiber pull-out and increased fiber/resin adhesion over the PPS# samples. The nickel coating on the graphite reinforcement lowered the tensile and impact properties (see table III and figure 7). This was caused by an overall decrease in the stress transfer from the resin to the fiber by poor interfacial bonding. This was seen with SEM in figure 8 where fiber/resin bonding is compared on two tensile fracture surfaces for nickel coated and uncoated fibers. The nickel coating or sheath inhibits chemical bonding between the fiber and the resin. The small improvement in electrical properties needs to be weighed against the decrease in mechanical properties.

Optical microscopy was used to examine the quality of the molding as well as the fiber distribution and orientation. Figure 9 and 10 show photomicrographs of 20 and 30% Gr/PEI and Gr/PPS. The PPS samples contained more voids which would contribute to their lower strength.

The 30% NiGr and Gr/PPS was found to contain an excessive amount of voids. This high void content was reflected by the low mechanical properties. Figure 11 shows a 40% Gr/PPS# photomicrograph of an injection molded chopped fiber composite. Notice the fiber orientation change through the thickness. The fibers tend to align in the same direction along the surfaces (mold walls) while a more random orientation occurs in the center. This sample came from the edge of a plate that was gated at its center point. Obviously the pattern will change depending on the location in the sample. If the same location is chosen for each sample then a fair comparison is possible. By using the reduced negative as a diffraction mask a pattern indicative of the overall orientation can be generated. Figure 12 shows the laser diffraction patterns for 20% and 40% Gr/PPS#. The higher fiber content has a more random distribution based on the shape of the pattern. This technique is good for comparing samples within a particular fiber content as well. Through comparisons with computer-generated standards a quantitative degree of orientation can be assessed. Figure 13 shows a series of diffraction patterns corresponding to various levels of orientation from computer-generated examples.

Processing conditions such as gate location, flow patterns, and resin viscosity as well as wall thickness and geometry dictate the degree of orientation. An attempt will be made to correlate this data with electrical conductivity and electromagnetic interference (EMI) attenuation in the future.

Scanning electron microscopy was also used to examine the as molded surfaces of the Ni Gr samples. Note in figure 14 the exposure of fiber on the rough resin surface. It is the non-uniformity of the exposed fibers that causes the inconsistency in resistivity measurements.

SUMMARY

A number of injection molded conductive fiber reinforced thermoplastics were characterized. The systems consisted of: A—30% NiGr/Nylon 66; 30% Gr/PEI; 12% SS/PPO; 35% Al flake/Nylon 66; 7% SS/PC; and 40% Gr/PPS, B—10, 20 and 30 weight percent Gr/PEI, C—10, 20, 30 and 40 weight percent Gr and NiGr reinforced PPS# and D—50 and 60 weight percent NiGr PPS#. Most of these materials A—D were supplied in molded plaque form or individually molded tensile specimens. Some of the tests such as drop weight impact testing or EMI measurements were conducted on full size plaques. Specimens were removed from the various plaque materials to conduct open circuit potential and galvanic couple corrosion rate measurements, assess effects of galvanic attack, measure moisture absorption, chemical resistance and conductivity. SEM and fiber orientation studies were also performed on specific specimens. Group A had the solvent resistance and conductivity measurements performed while group D only had electrical resistivity tests conducted on full size plaques. The remaining groups had all the aforementioned tests conducted including tensile testing.

The 40 weight percent Ni coated Gr provided the most conductive composites. Plating the thermoplastic plaques brought EMI attenuation readings up to that of bare aluminum. Various potential measurements indicated the possibility of galvanic corrosion between aluminum and Gr reinforced thermoplastics. The LCP and to a lesser degree PPS# material showed the best resistance to various solvents. The tensile strength and strain to failure of the PEI material was higher than the PPS, and this was true for drop weight impact tests which were based on through penetration. The Ni coating on the Gr although enhancing conductivity, lowered tensile and impact properties by causing a decrease in stress transfer from resin to fiber. Laser diffraction data permitted a quantitative assessment of fiber orientation and the possibility of correlation with electrical and mechanical properties.

FUTURE EFFORTS

Additional work should be performed with different fiber forms, in various combinations, to improve electrical properties of the chopped fiber composites. New tough solvent resistance thermoplastics should be investigated as matrix materials. Effort should be devoted to experimental configurations of promising conductive composite systems such as enclosures or black boxes for aircraft applications. Quantitative correlation of orientation with electrical and mechanical properties in chopped fiber composites would be extremely beneficial and should be actively pursued.

TABLE I
Operational and Maintenance Chemicals

Designation	Specification
Mineral Spirits	TT-T-281
Naphtha (aromatic)	TT-N-97
Naphtha (aliphatic)	TT-N-95
Remover, Paint, Epoxy and Polyurethane Systems	MIL-R-81294
MEK	TT-M-261
Cleaning Compounds, Aircraft Surfaces 10% in Water	MIL-C-43416 Class 1
Coolanol 25R Heat Transfer Fluid	—
Lubricating Oil	MIL-L-6085
Lubricating Oil	MIL-L-23699
Hydraulic Fluid	MIL-H-5606
Hydraulic Fluid	MIL-H-83282
Turbine Fuel JP-5	MIL-T-56240

TABLE II
Electrical and Electrochemical Properties

Material	Volume Resistivity ohm-cm	Rest Potential mV	Zero Impedance Galvanic Current $\mu A/cm^2$
PPS# + 10% Gr	10 ⁵	57	8
PPS# + 10% NiGr	10 ³	-260	1.5
PPS# + 20% Gr	10 ³	50	12
PPS# + 20% NiGr	—	—	—
PPS# + 30% Gr	10 ²	+ 45	25
PPS# + 30% NiGr	10 ¹	-260	50
PPS# + 40% Gr	10 ¹	+105	26
PPS# + 40% NiGr	10 ⁰	-200	85
PPS# + 50% NiGr	10 ⁰	—	—
PPS# + 60% NiGr	10 ⁰	—	—
PEI + 10% Gr	10 ³		
PEI + 20% Gr	10 ³		
PEI + 30% Gr	10 ³	- 78	16
Nylon 6/6 + 30% NiGr	10 ¹	-200	1.2
Nylon 6/6 + 35% AL	10 ⁵		
LCP + 40% Gr	10 ²	-145	28
PPO + 12% SS	10 ⁴	+100	4.7
PC + 7 SS	10 ²	+110	1.4
AL (2024-T3)	10 ⁻⁶	-790	
AL (7075-T65)	10 ⁻⁶	-780	

TABLE III
Tensile & Impact Properties of Chopped Fiber
Filled PPS & PEI

MATERIAL	MAX. ABSORBED ENERGY (Ft.-lbs) (JOULES)	TENSILE STRENGTH (psi) (MPa)	TENSILE MODULUS (Ksi) (GPa)	STRAIN TO FAILURE (%)
PPS# + 10% Gr	4.28 (5.8)	9070 (62.5)	530 (3.6)	1.71
PPS# + 10% NiGr	3.39 (4.6)	8880 (61.2)	567 (3.9)	1.58
PPS# + 20% Gr	9.66 (13.1)	10,700 (73.8)	860 (5.9)	1.21
PPS# + 30% Gr	10.98 (14.9)	5340 (36.8)	820 (5.6)	0.67
PPS# + 30% NiGr	4.34 (5.9)	7720 (53.2)	1180 (8.1)	0.68
PPS# + 40% Gr	10.64 (14.4)	14,920 (102.9)	2270 (15.6)	0.67
PPS# + 40% NiGr	5.25 (7.1)	6710 (46.3)	1640 (11.3)	0.42
PEI, 10% Gr	9.37 (12.7)	22,200 (153.0)	930 (6.4)	2.4
PEI, 20% Gr	8.96 (12.1)	25,220 (173.8)	1670 (11.5)	1.54
PEI, 30% Gr	14.39 (19.5)	30,560 (210.7)	2420 (16.7)	1.38

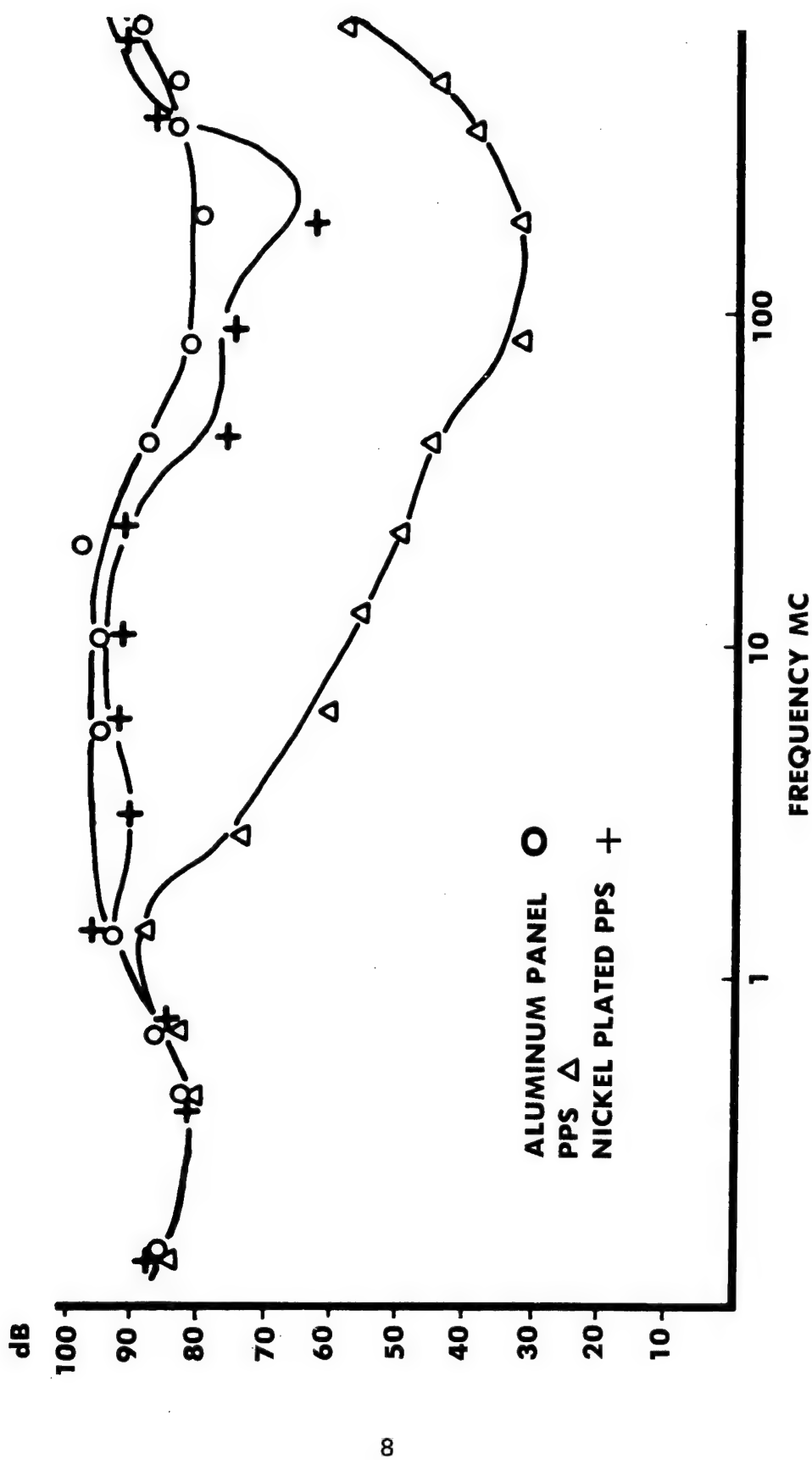


Figure 1. Plot of EMI Attenuation (vs. frequency) Comparing Nickel Plated Plated PPS (40% Gr), uncoated PPS (40% Gr), and Aluminum

NADC-84054-60

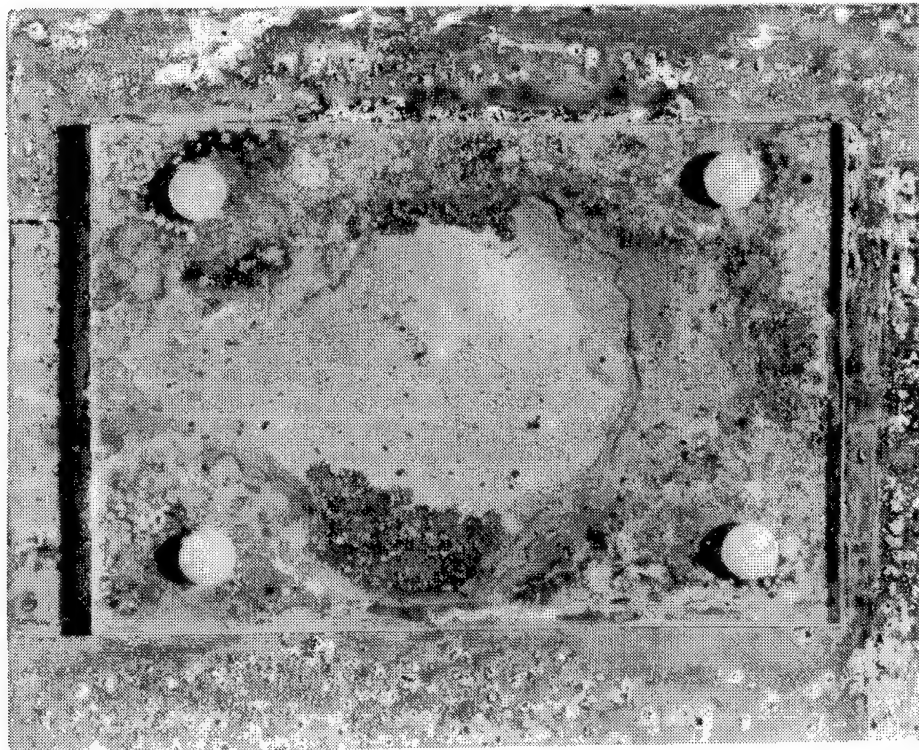
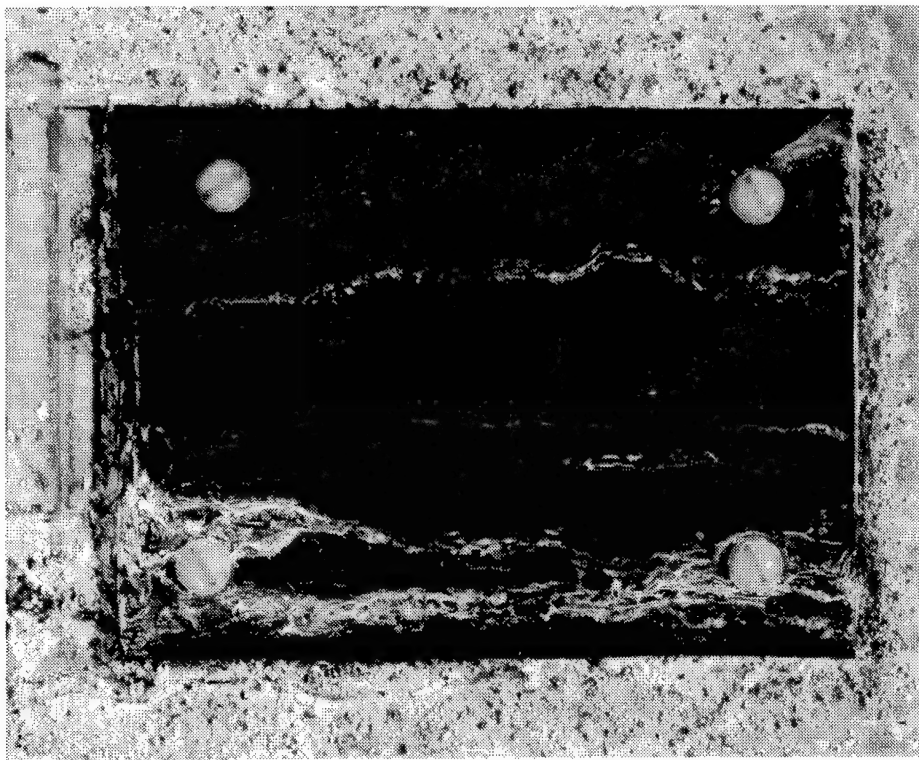


Figure 2. Comparison of Galvanic Couples (40% Gr/PPS vs. Acrylic) Exposed to Salt Fog

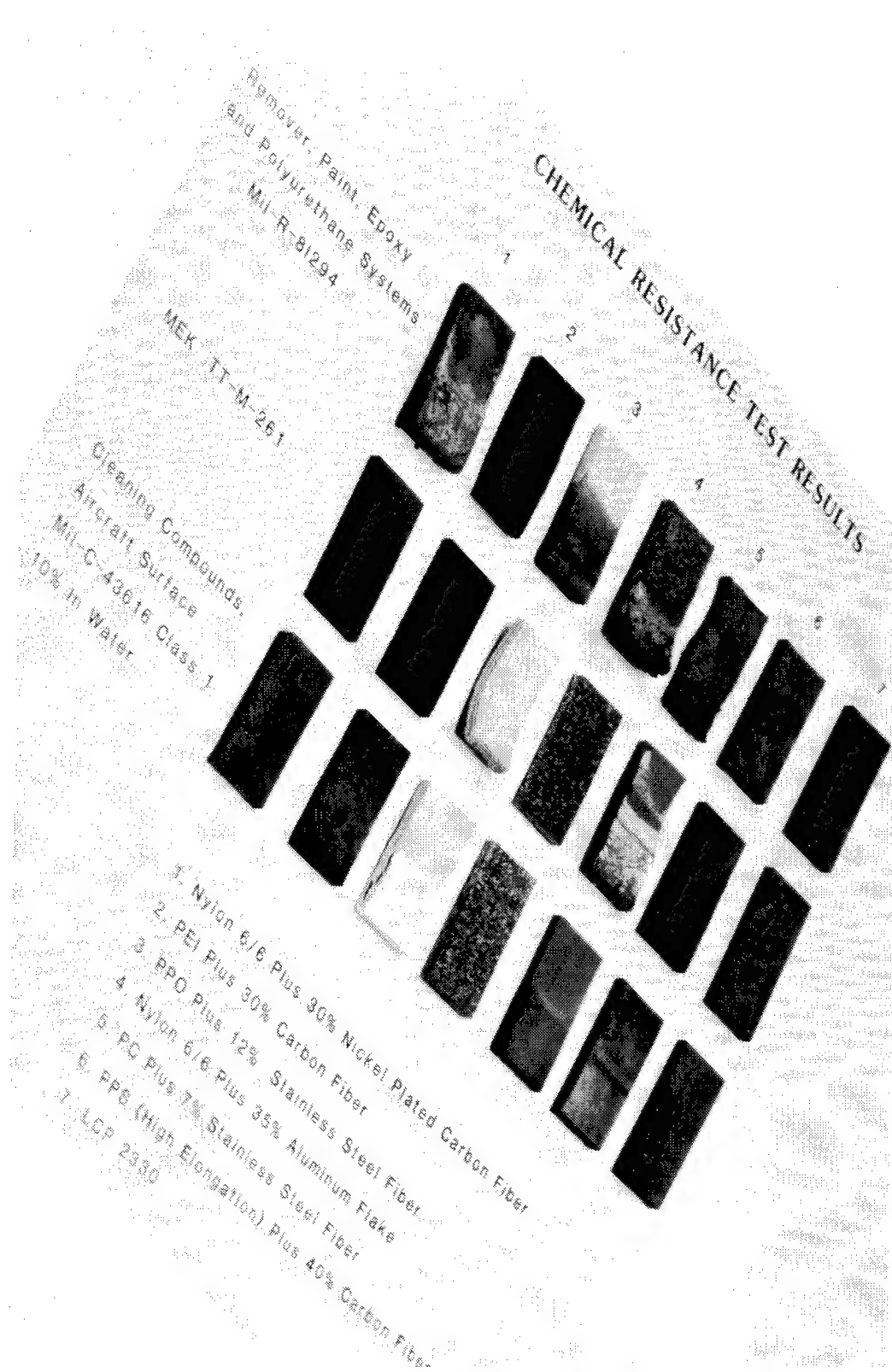


Figure 3. Effects of the Three Harshest Solvents After One Week Immersion

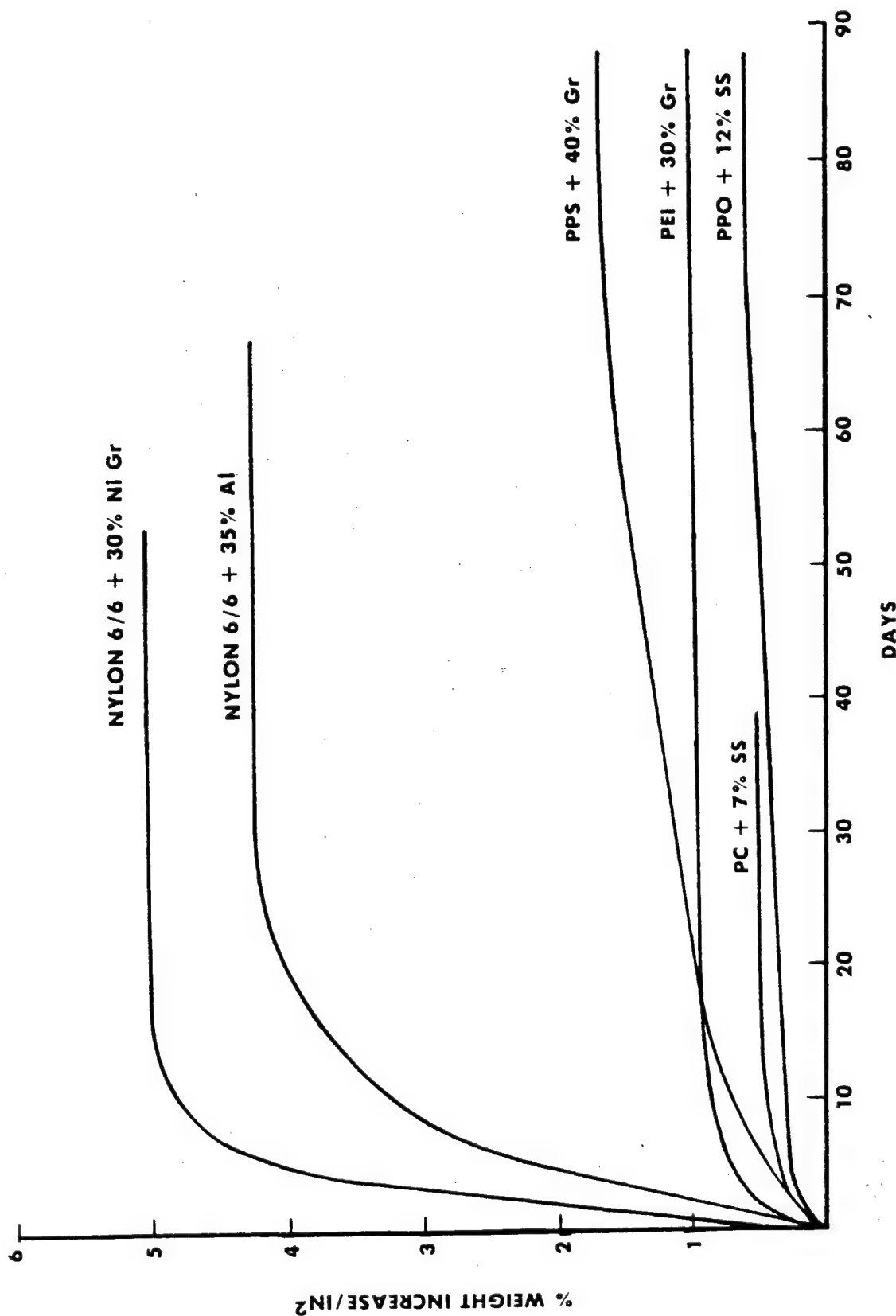


Figure 4. Plots of Water Absorption vs. Time for Various Components

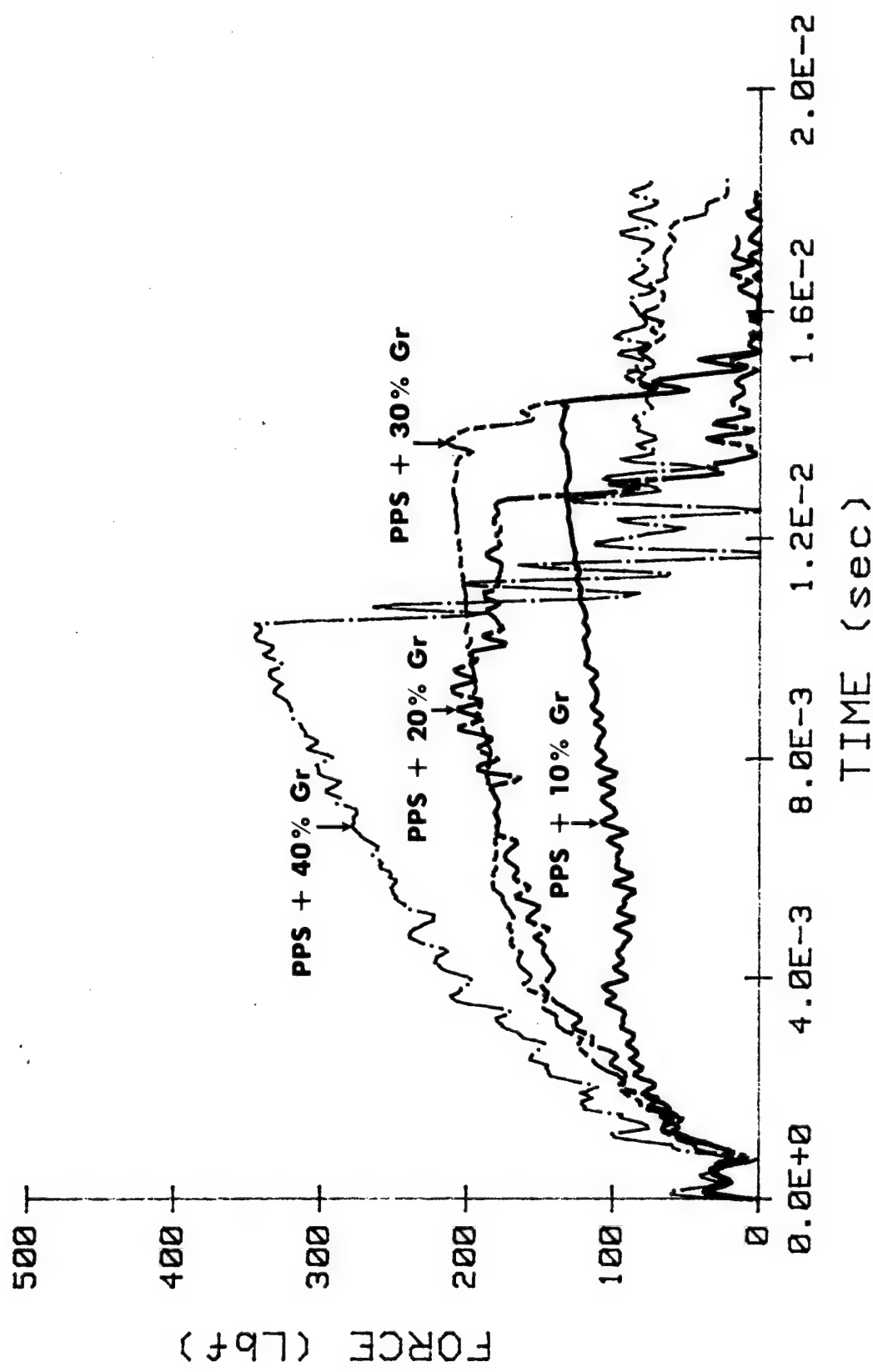
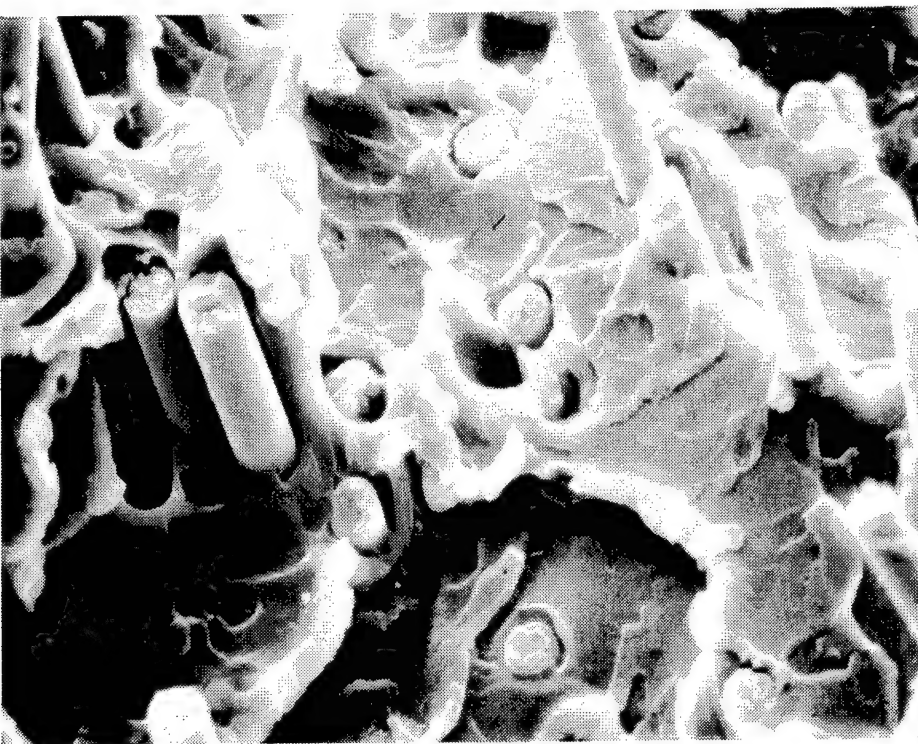
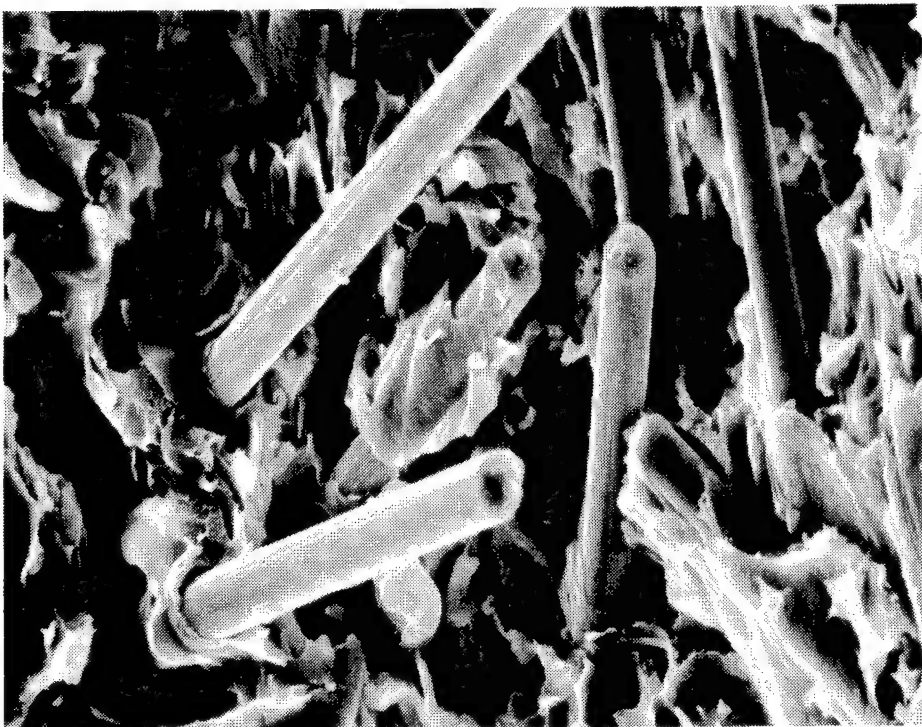


Figure 5. Force vs. Time Plots of Several Drop-Weight Impact Tests for Gr/PPS (10%, 20%, 30% and 40% Gr)



PEI



PPS

Figure 6. SEM Photographs of 20% Gr/PPS and PEI Tensile Fracture Surfaces (1000X)

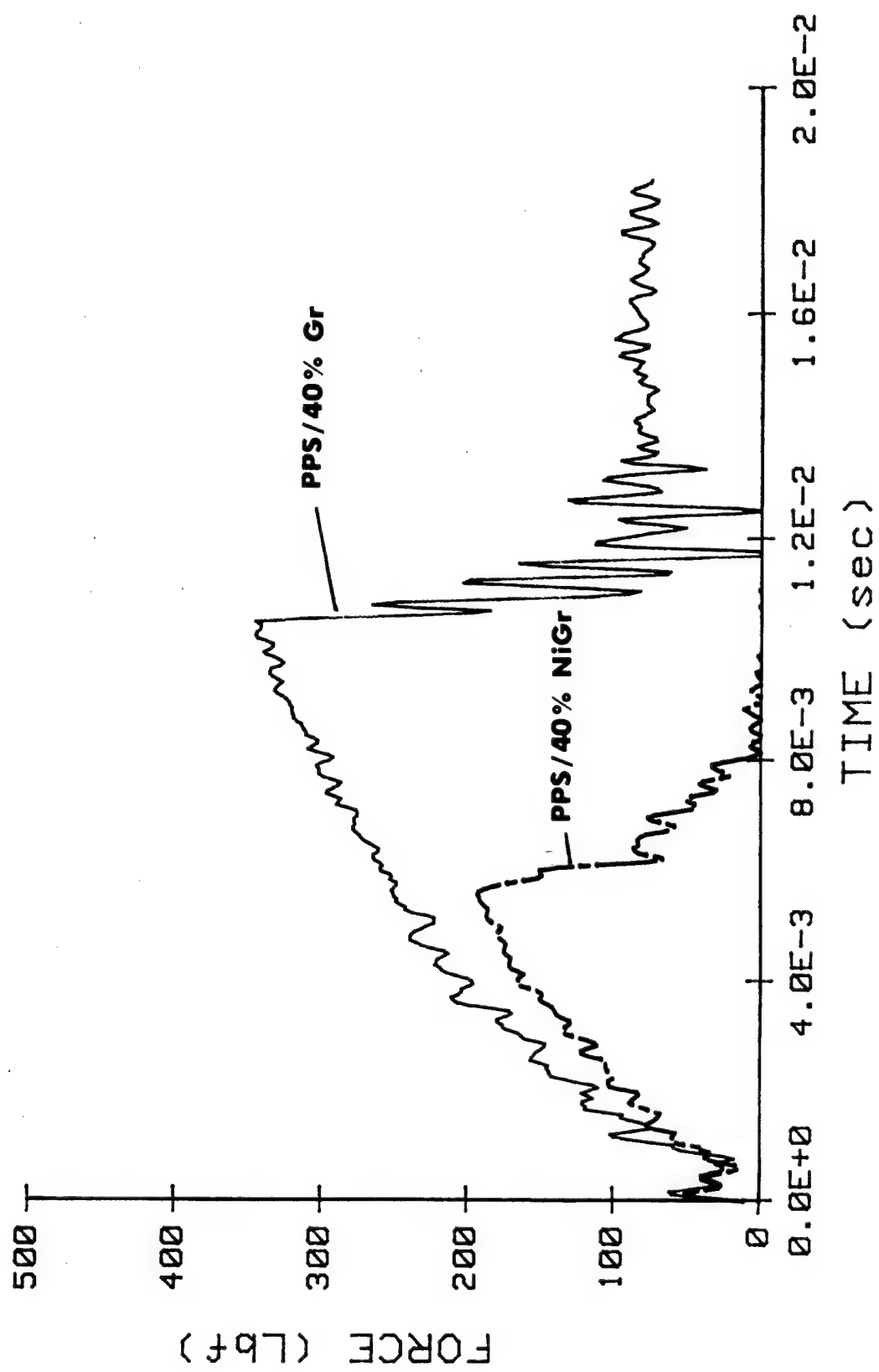
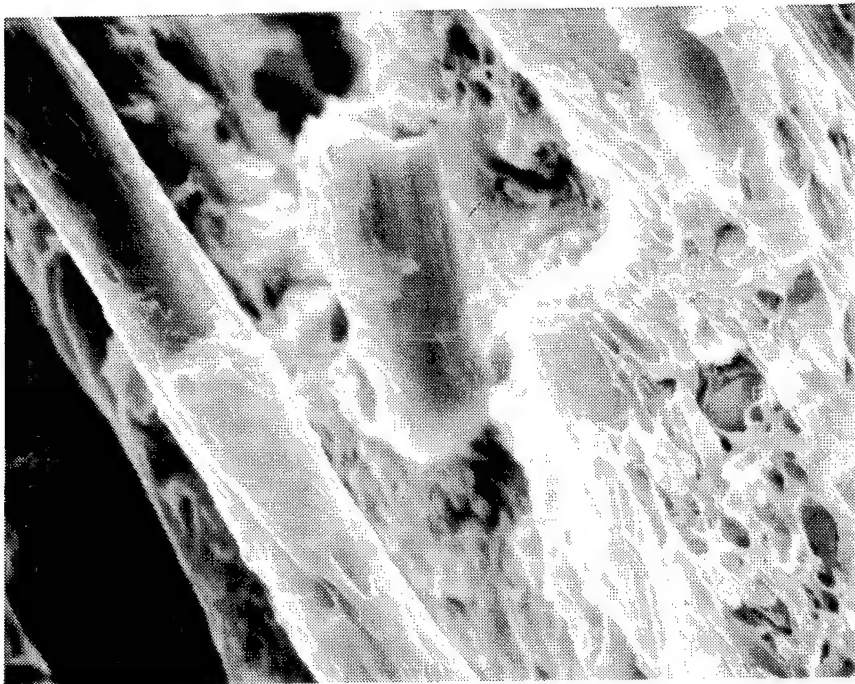
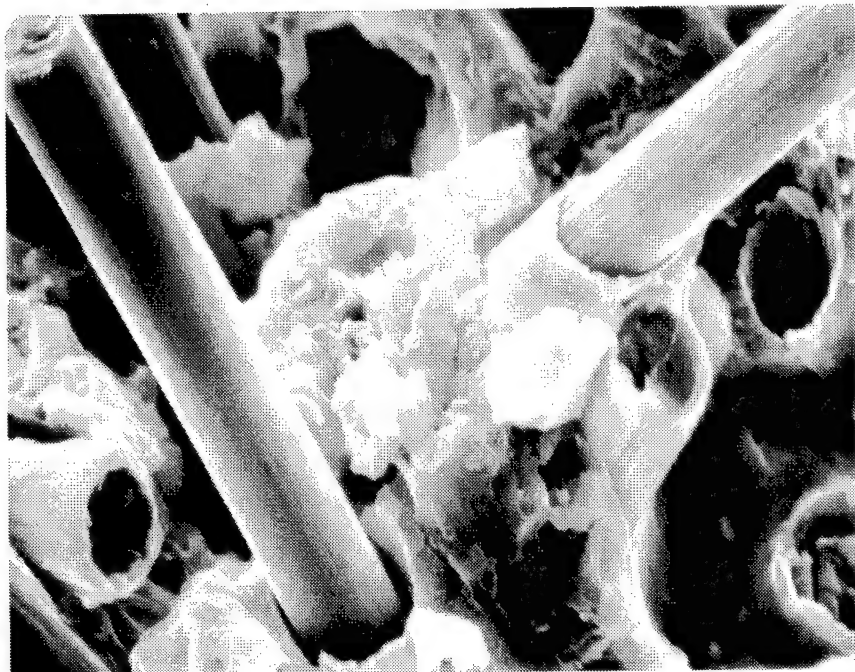


Figure 7. Force vs. Time Plots of 40% Gr and NiGr PPS From Drop-Weight Impact Tests

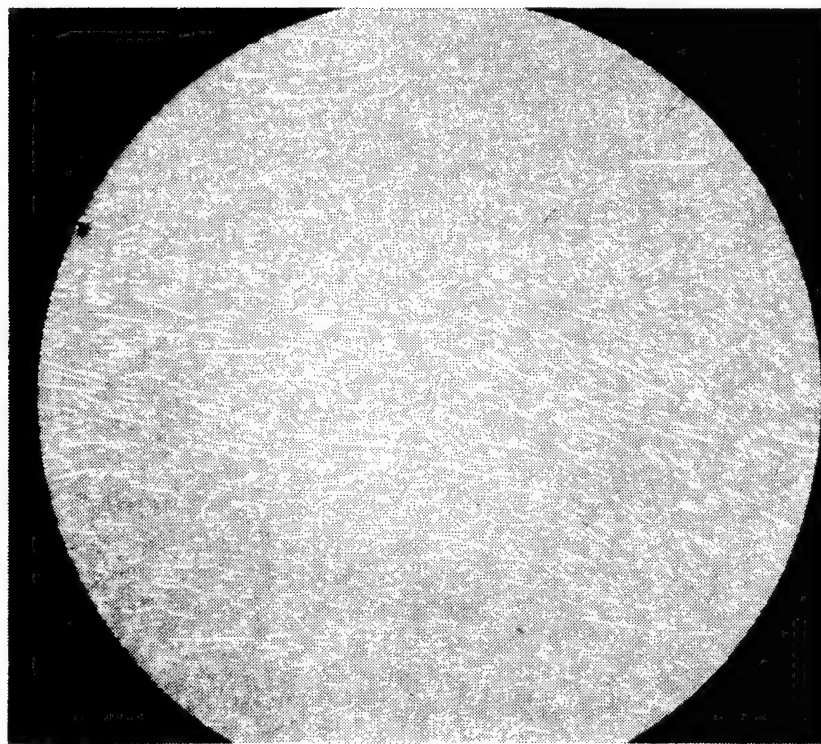


40% GR/PPS

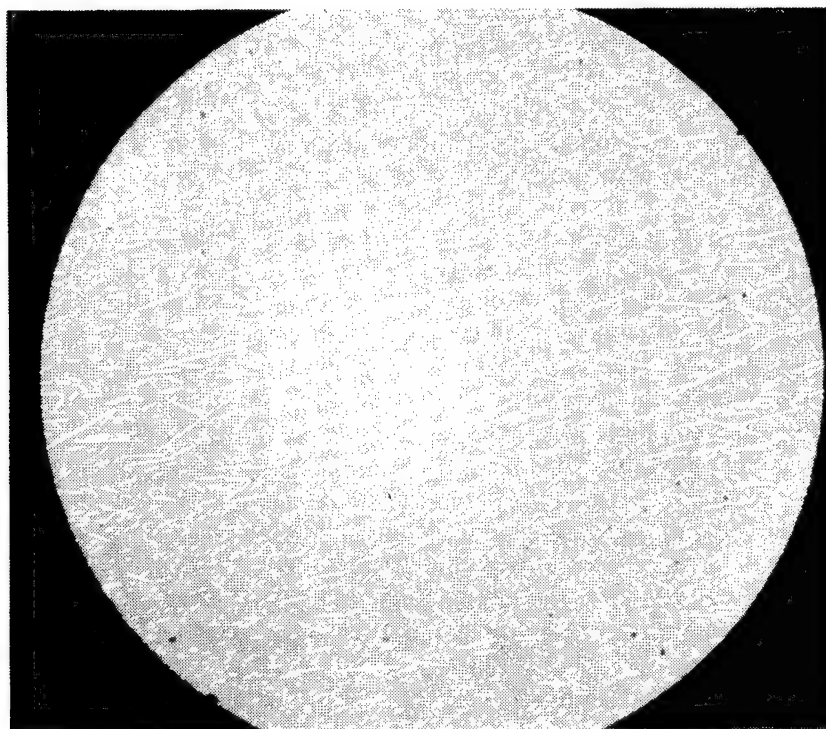


40% NiGR/PPS

Figure 8. SEM Photographs of 40% Gr and NiGr/PPS Tensile Fracture Surfaces (20000X)

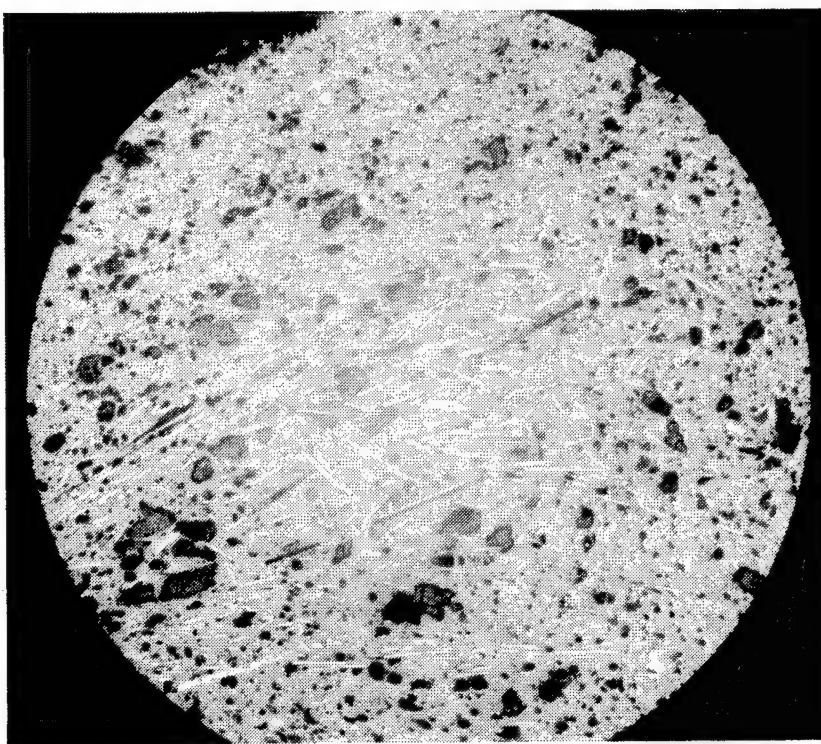


30% Gr

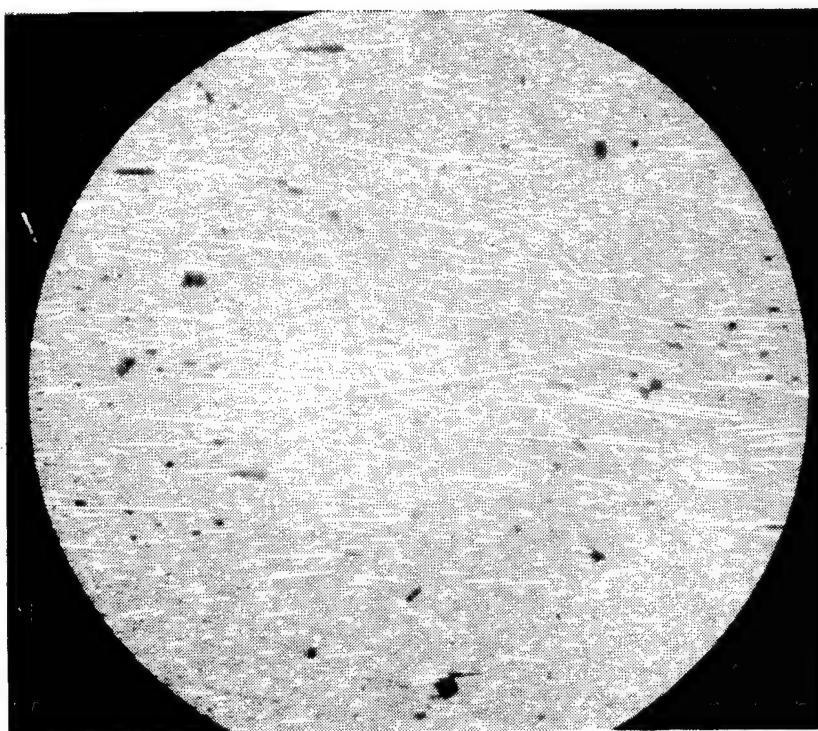


20% Gr

Figure 9. Photomicrographs (50X) of 20% and 30% Gr/PEI



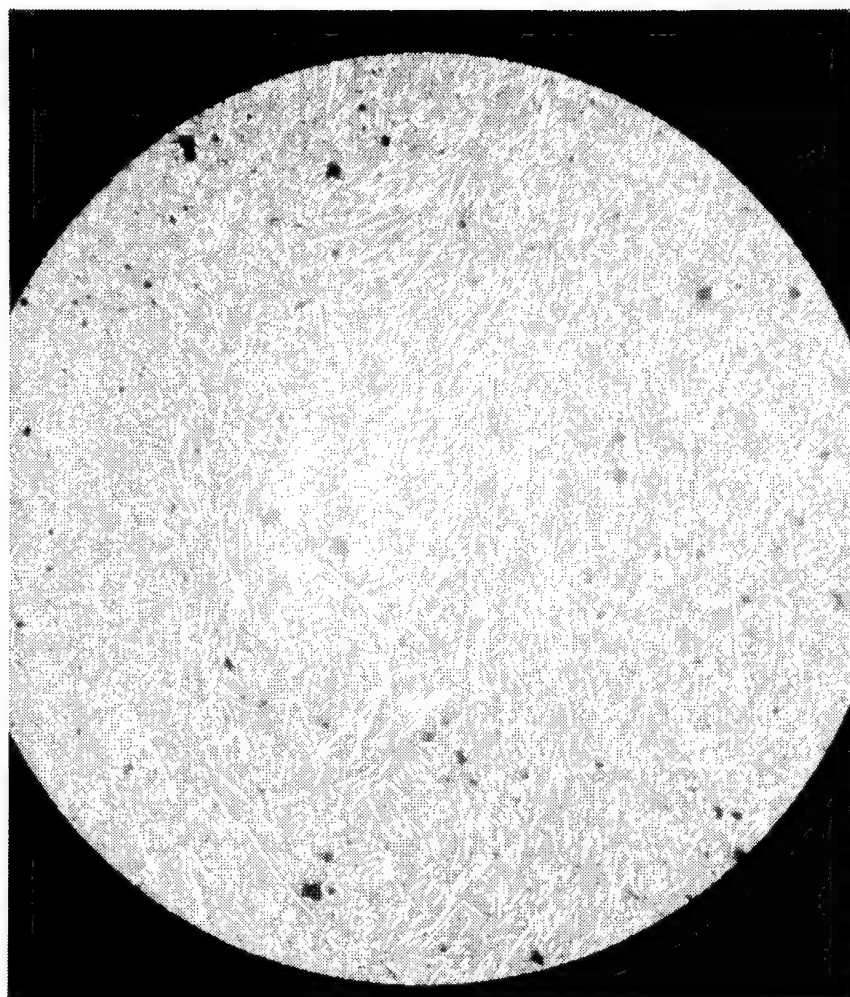
30% Gr



20% Gr

Figure 10. Photomicrographs (50X) of 20% and 30% Gr/PPS

NADC-84054-60



40% Gr/PPS

Figure 11. Photomicrograph (50X) of 40% Gr/PPS

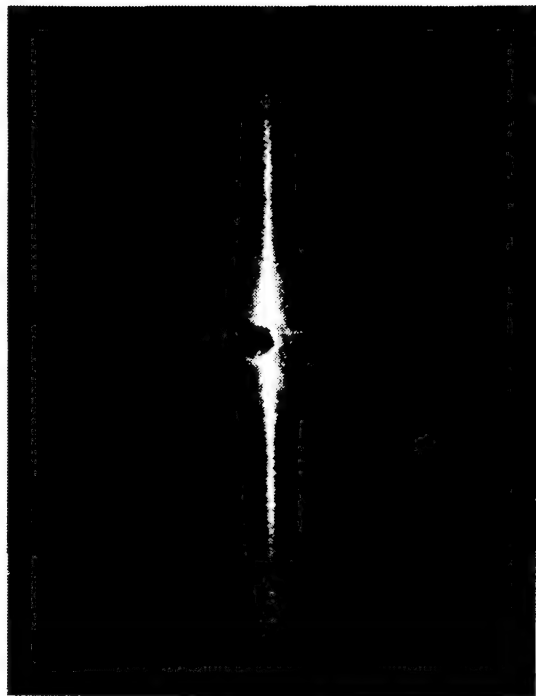


20%

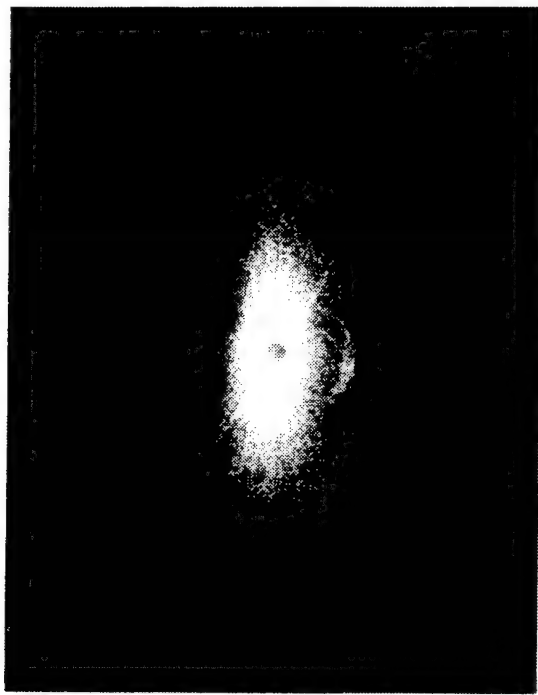


40%

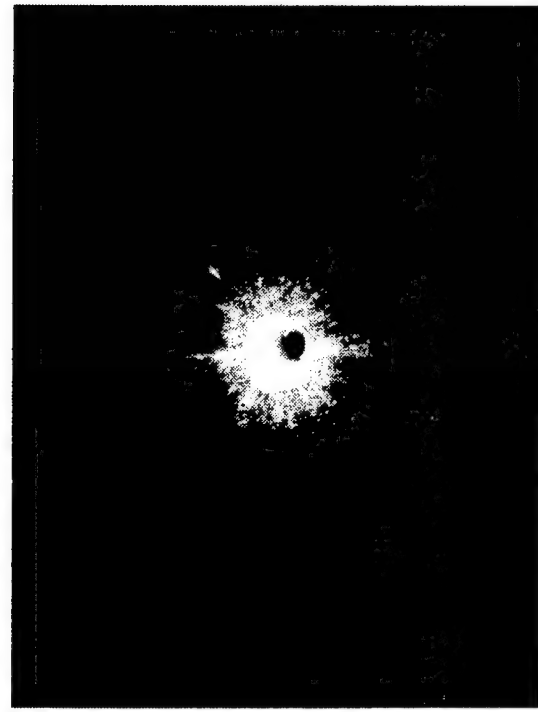
Figure 12. Laser Diffraction Patterns for 20% and 40% Gr/PPS



PERFECTLY ORIENTED



INTERMEDIATE



RANDOM

Figure 13. Series of Laser Diffraction Patterns Corresponding to Various Levels of Orientation

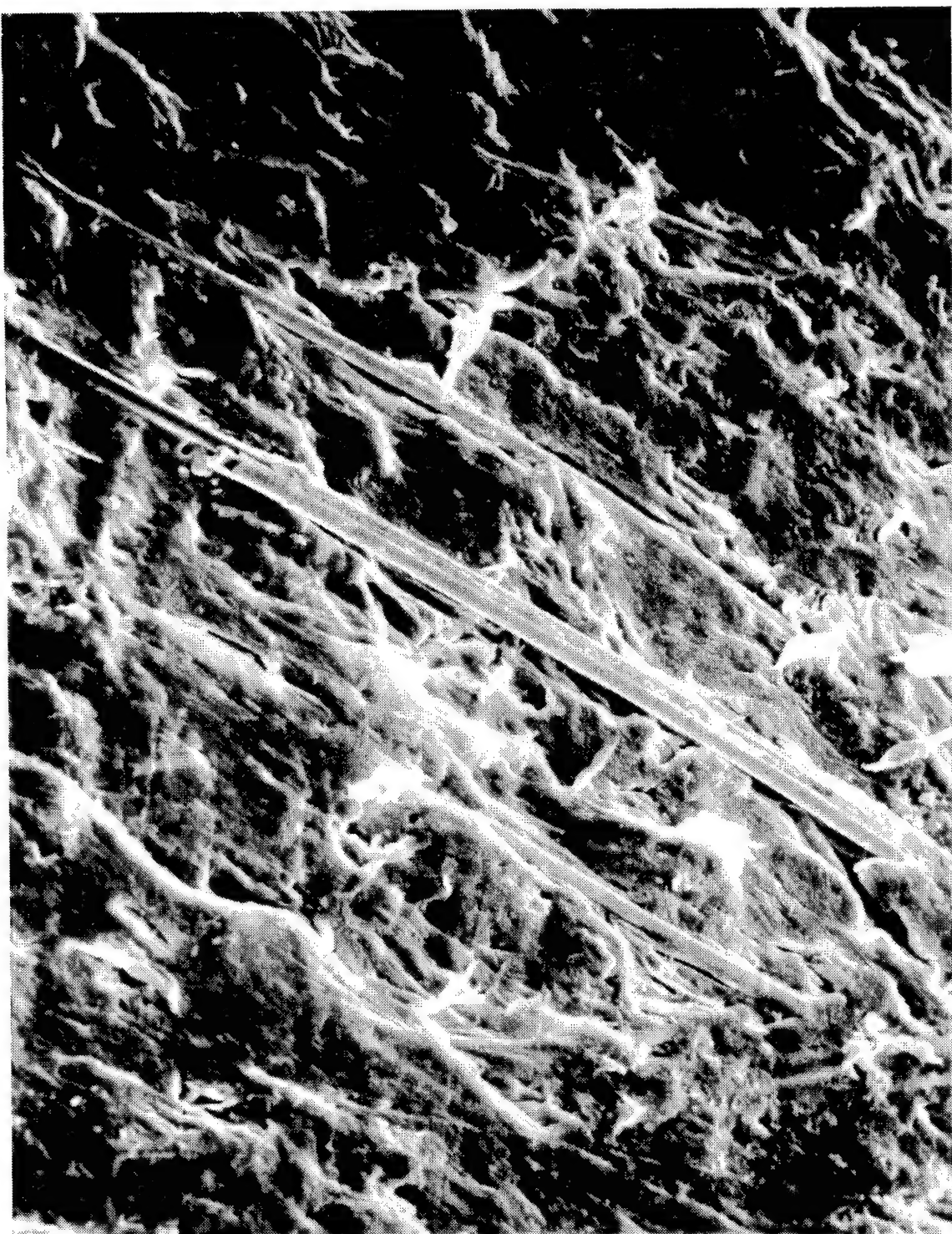


Figure 14. SEM Photograph of NiGr Fibers on the As-Molded Surface (200X)

ACKNOWLEDGEMENTS

The authors wish to thank E. Lyon, D. Heal, M. Oliveto, and J. Thompson for their fine contributions to this work.

REFERENCES

1. Shaffer, I. & Trabocco, R. "The Use of Conductive Thermoplastic Composites for Aircraft Electrical Connector Shells," NADC Tech. Mem. No. ACSTD-TM-2087 of 11 May 1981.
2. Bigg, D. M., "Mechanical, Thermal & Electrical Properties of Metal Fiber-Filled Polymer Composites," Polymer Engr. & Sciences, Dec. 1979, Vol. 19, No. 16
3. Simon, R. M., "EMI Shielding Can Be Made of Conductive Plastics," Ind. Res & Dev., 1982, P. 104.
4. Bradish, F. W., "Conductive SMC/BMC Composites for RFI/EMI Shielding," SPI 33rd Annual Tech Conf. 1978.
5. Fischer, P. and DeLuccia, J "Effects Of Graphite-Epoxy Composite Materials On The Corrosion Behavior Of Aircraft Alloys," Naval Air Development Center Report No. NADC-75031-30, April 1975.
6. Weber, K. E. and al "Corrosion Problems Associated with Filamentary Composites in Contact with Metals," AFML Advanced Composites Review, April 1970.

DISTRIBUTION LIST (CONTINUED)

REPORT NO. NADC-84054-60

	<u>No. of Copies</u>
Plastics Technical Evaluation Center	1
ARRADCOM	
Bldg. 351-N	
Dover, NJ 07801	
Attn: A. M. Anzalone	
Massachusetts Institute of Technology	1
Cambridge, MA	
Attn: D. Roylance	
G. Wnek	
CIBA Geigy Corporation	1
Ardsley, NY 10502	
Attn: J. Weiss	
Martin Marietta	1
Tech Library	
Orlando, FL	
Sacramento Air Logistics Center/MME	1
Advanced Composite Program Office	
McClellan AFB, CA 95652	
Attn: Lt. Col. Bradley	
Defense Technical Information Center	12
Attn: DTIC-DDA-1	
Cameron Station, Bldg. 5	
Alexandria, VA 23314	
NAVAIRDEVCEC	23
(3 for Code 8131)	
(20 for Code 6063)	

DISTRIBUTION LIST (CONTINUED)

REPORT NO. NADC-84054-60

	<u>No. of Copies</u>
United Aircraft Corp.	1
Pratt & Whitney Aircraft Division East Hartford, CT 06108	
United Aircraft Corp.	1
Sikorsky Aircraft Division Stratford, CT 06602 Attn: Mr. J. Ray	
United Carbide Corp.	1
Carbon Products Division P.O. Box 6116 Cleveland, OH 44101	
University of Maryland	1
College Park, MD 20742 Attn: Dr. W. J. Bailey	
Naval Air Rework Facility	1
Mail Stop No. 9 MCAS Cherry Point, NC 28533 Attn: T. Fuss, Code 343 D. Steiniger, Code 343	
University of Wyoming	1
Mechanical Engineering Dept. Laramie, WY 82071 Attn: Dr. D. F. Adams	
Army Materials & Mechanics Research Center	1
Polymers & Chemistry Div. Watertown, MA 02172 Attn: G. L. Hagnauer R. E. Sacher	
Hercules, Inc.	1
Magna, UT 84044 Attn: R. E. Hoffman N. Bascom	
General Electric Co.	1
Mail Stop No. 89 Cincinnati, OH 45215 Attn: Max Grandey	

DISTRIBUTION LIST (CONTINUED)

REPORT NO. NADC-84054-60

	<u>No. of Copies</u>
General Dynamics	1
Convair Aerospace Division P.O. Box 748 Fort Worth, TX 76101 Attn: Tech. Library	
General Dynamics	1
Convair Division P.O. Box 1128 San Diego, CA 92138 Attn: Mr. W. Scheck, Dept. 572-10	
TRW, Inc.	1
Systems Group One Space Park Bldg. No. 1, Room 2171 Redondo Beach, CA 90278	
McDonnell Douglas Corp.	1
McDonnell Aircraft Co. P.O. Box 516 St. Louis, MO 63166 Attn: Mr. R. Juergens Dr. J. Carpenter	
Fibers Material Inc.	1
Biddeford Industrial Park Biddeford, ME 04005 Attn: Mr. J. Herrick	
Rockwell International Science Center	1
P.O. Box 1085 Thousand Oaks, CA 91360 Attn: C. Hammermesh	
David W. Taylor R&D Center	1
Bethesda, MD 20084 Attn: Mr. M. Krenzke, Code 1730	
NASA	1
Langley Research Center Hampton, VA Attn: B. Stein	
United Aircraft Corp.	1
United Aircraft Research Labs E. Hartford, CT 06108	

DISTRIBUTION LIST (CONTINUED)

REPORT NO. NADC-84054-60

	<u>No. of Copies</u>
General Electric Company	1
Valley Forge Center Philadelphia, PA 19101	
Monsanto Research Corp.	1
1777 Walton Road Blue Bell, PA 19422 Attn: W. Rosen	
U. S. Army Air Mobility R&D Laboratory	1
Fort Eustis, VA 23604 Attn: SAVDL-EU-SS	
B. F. Goodrich Aerospace and Defense Products	1
500 South Main Street Akron, OH 44318	
Lockheed California Co.	1
Box 551 Burbank, CA 91520 Attn: Mr. J. H. Wooley	
Lockheed-Georgia Co.	1
Marietta, GA 30063 Attn: Mr. L. E. Meade	
Lockheed Missiles & Space Co.	1
Sunnyvale, CA 94088 Attn: Mr. H. H. Armstrong, Dept. 62-60	
TRW, Inc.	1
23555 Euclid Ave. Cleveland, OH 44117	
E. I. Dupont de Nemours & Co.	1
Textile Fibers Dept. Wilmington, DE 19898	
Bell Aerospace Co.	1
Buffalo, NY 14240 Attn: Mr. F. M. Anthony	
Union Carbide Corp.	1
Chemicals & Plastics One River Road Bound Brook, NJ	

DISTRIBUTION LIST (CONTINUED)

REPORT NO. NADC-84054-60

	<u>No. of Copies</u>
Air Force Materials Laboratory	5
Wright-Patterson Air Force Base	
Dayton, OH 45433	
Attn: Codes LC (1)	
LN (1)	
LTF (1)	
LAE (1)	
MBC (1)	
Air Force Dynamics Laboratory	1
Wright-Patterson Air Force Base	
Dayton, OH 45433	
Attn: Code FDTC	
Defense Ceramic Information Center	1
Battelle Memorial Institute	
505 King Ave.	
Columbus, OH 43201	
Illinois Institute of Technology	1
Research Institute	
10 West 35th Street	
Chicago, IL 60616	
Attn: Dr. E. Hofer	
Acurex	1
Aerospace Systems Division	
485 Clyde Ave.	
Mountain View, CA 94042	
Attn: R. M. Washburn	
Grumman Aerospace Corp.	
Bethpage, NY 11714	
Attn: J. Mahon	
HITCO	1
1600 W. 135th St.	
Gardena, VA 90406	
ACVO Corp.	1
Applied Technology Division	
Lowell, MA 01851	
McDonnell-Douglas Corp.	3
P.O. Box 516	
St. Louis, MO 63166	
Attn: Dr. C. Lind	
K. Westphal	
G. Boguki	

DISTRIBUTION LIST (CONTINUED)

REPORT NO. NADC-84054-60

	<u>No. of Copies</u>
Naval Ship Engineering Center	1
Code 6101E	
Navy Department	
Washington, DC 20360	
Vought Corporation	1
P. O. Box 5907	
Dallas, TX 75222	
Attn: R. Knight	
NASA Headquarters	1
Code RV-2 (Mr. N. Mayer)	
600 Independence Ave., S.W.	
Washington, DC 20546	
Boeing-Vertol Co.	1
P.O. Box 16858	
Philadelphia, PA 19152	
Attn: Dept. 1951	
Boeing Aerospace Co.	1
P. O. Box 3999	
Seattle, WA 98124	
Attn: C. Sheppard	
Naval Air Systems Command	5
Washington, DC 20361	
Attn: Code AIR-5304C	
Office of Naval Research	1
Code 472	
Washington, DC 20350	
Office of Naval Research, Boston .	1
495 Summer Street	
Boston, MA 02210	
NAVAL GENERAL LIBRARIES	
Naval Research Laboratory	2
Codes 6306 and 6120	
Washington, DC 20350	
Chief of Naval Education	
and Training	
NAVEDTRA 5070/2 (Rev. 9-80) S/N 0115-LF-050-7022	
Naval Surface Weapons Center ...	1
Code 234	
White Oak, Silver Spring, MD 20910	